Archives of Toxicology (2020) 94:3157–3171
https://doi.org/10.1007/s00204-020-02811-5

MOLECULAR TOXICOLOGY

Targeting organophosphorus compounds poisoning by novel quinuclidine-3 oximes: development of butyrylcholinesterase-based bioscavengers

Antonio Zandona[1] · Maja Katalinić[1] · Goran Šinko[1] · Andreja Radman Kastelic[2] · Ines Primožič[2] · Zrinka Kovarik[1]

Received: 29 April 2020 / Accepted: 15 June 2020 / Published online: 24 June 2020

Abstract

A library of 14 mono-oxime quinuclidinium-based compounds with alkyl or benzyl substituent were synthesized and characterized in vitro as potential antidotes for organophosphorus compounds (OP) poisoning treatment. We evaluated their potency for reversible inhibition and reactivation of OP inhibited human acetylcholinesterase (AChE) and butyrylcholinesterase (BChE) and evaluated interactions by molecular docking studies. The reactivation was notable for both AChE and BChE inhibited by VX, cyclosarin, sarin and paraoxon, if quinuclidinium compounds contained the benzyl group attached to the quinuclidinium moiety. Out of all 14, oxime **Q8** [4-bromobenzyl-3-(hydroxyimino)quinuclidinium bromide] was singled out as having the highest determined overall reactivation rate of approximately 20,000 M^{-1} min^{-1} for cyclosarin-inhibited BChE. Furthermore, this oxime in combination with BChE exhibited a capability to act as a bioscavenger of cyclosarin, degrading within 2 h up to 100-fold excess of cyclosarin concentration over the enzyme. Molecular modeling revealed that the position of the cyclohexyl moiety conjugated with the active site serine of BChE directs the favorable positioning of the quinuclidinium ring and the bromophenyl moiety of **Q8**, which makes phosphonylated-serine easily accessible for the nucleophilic displacement by the oxime group of **Q8**. This result presents a novel scaffold for the development of new BChE-based bioscavengers. Furthermore, a cytotoxic effect was not observed for **Q8**, which also makes it promising for further in vivo reactivation studies.

Keywords Aldoxime · Antidote · Nerve agents · Bioscavenging · Reactivation · Cytotoxicity

Introduction

People are exposed to organophosphorus compounds (OP) in everyday life, from industry to agronomy and their accidental or deliberate intake still accounts for a great number of poisonings worldwide (Gunnell et al. 2017; Eddleston 2019). Furthermore, some OP are still a threat as chemical warfare agents (Fig. 1; e.g., tabun, sarin, soman, VX), even though the international OPCW Convention prohibited their production and development for that purpose (https://www.opcw.org). This danger was confirmed again as we witnessed attacks in Syria (with sarin) and the UK (with Novichok) (Dolgin 2013; Vale et al. 2018).

The high toxicity of all OP arises from the irreversible inhibition of acetylcholinesterase (AChE, EC 3.1.1.7), which consequently leads to the accumulation of acetylcholine in synapses, and thus disruption of nerve impulse transmission in the central and peripheral nervous system

✉ Maja Katalinić
mkatalinic@imi.hr

Antonio Zandona
azandona@imi.hr

Goran Šinko
gsinko@imi.hr

Andreja Radman Kastelic
radman.andreja@gmail.com

Ines Primožič
ines.primozic@chem.pmf.hr

Zrinka Kovarik
zkovarik@imi.hr

1 Institute for Medical Research and Occupational Health, Ksaverska cesta 2, 10001 Zagreb, Croatia

2 Department of Chemistry, Faculty of Science, University of Zagreb, Horvatovac 102A, 10001 Zagreb, Croatia

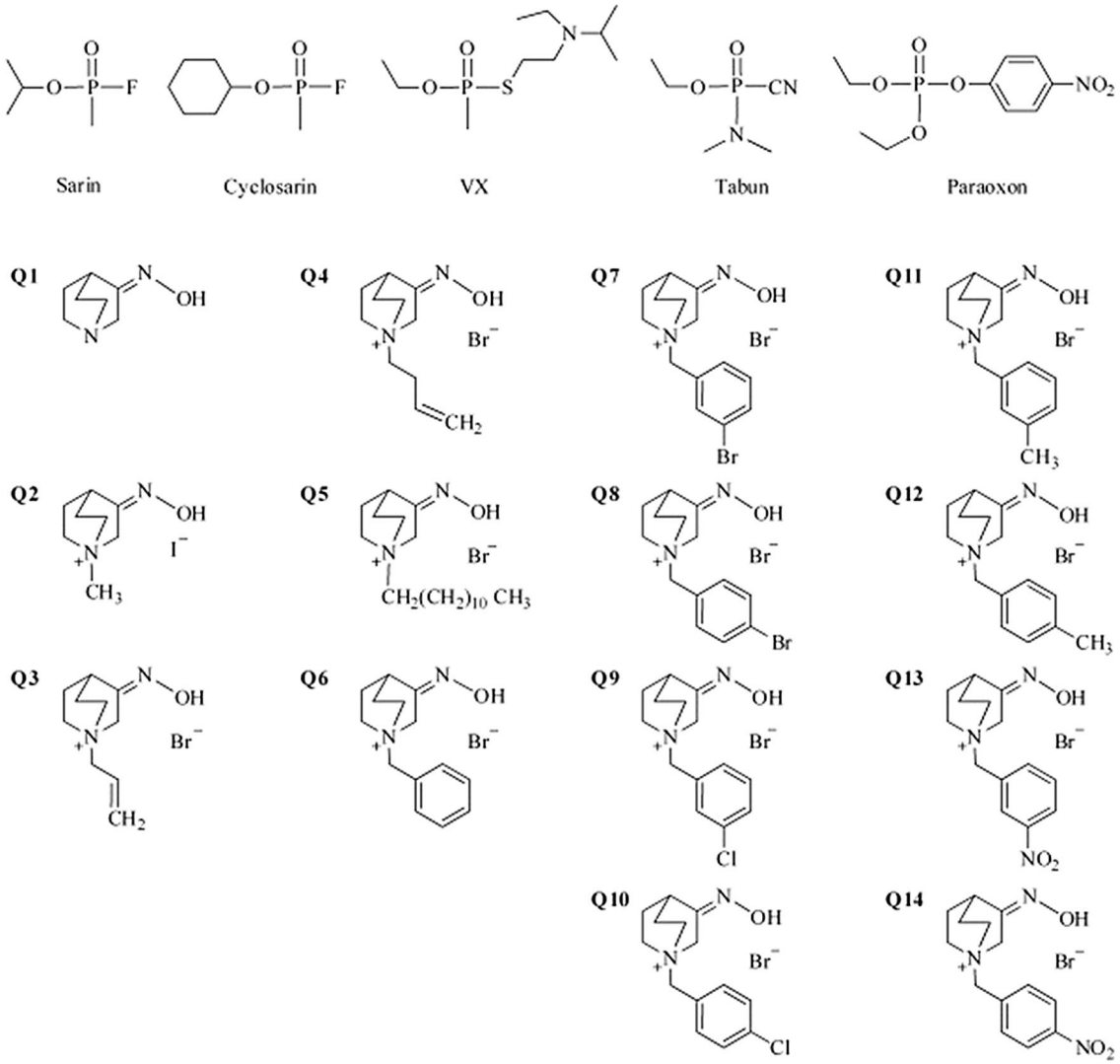

Fig. 1 The structures of OP used in this study and tested quinuclidinium oximes (**Q1**–**Q14**)

(Timperley et al. 2019). The therapy used today against OP poisoning involves the administration of compounds called oximes as reactivators of inhibited AChE (Hulse et al. 2019; Timperley et al. 2019). Since therapy-approved oximes (i.e., 2-PAM, HI-6 or obidoxime) have limitations, the search for new, more efficient ones is still a necessity. In addition, the researchers have found that the administration of enzymes capable of scavenging OPs can also help the outcome of treatment (Gupta et al. 2011; Melzer et al. 2012; Nachon et al. 2013; Ashani et al. 2016). In that sense, the naturally present plasma butyrylcholinesterase (BChE, EC 3.1.1.8) has been shown to be the most suitable for such studies (Masson and Lockridge 2010; Vučinić et al. 2013; Wille et al. 2019). BChE is an enzyme related to AChE, it acts as a stoichiometric scavenger capable of neutralizing OP before it reaches and inhibits AChE in the central nervous system. If continuously reactivated by oximes, BChE could neutralize higher doses of OPs in circulation, acting as a pseudo-catalytic agent (Kovarik et al. 2010a; Saxena et al. 2011; Radić et al. 2013a; Wille et al. 2019). However, inhibited BChE is resistant to reactivation with most oximes capable to reactivate inhibited AChE (Kovarik et al. 2008b, 2010b; Čalić et al. 2008; Zorbaz et al. 2018a). Therefore, the search to find an efficient oxime that would reactivate both inhibited cholinesterases is still a challenge.

It is known from previous studies that quinuclidinium compounds block the uptake mechanism of choline in the synaptic cleft; reduce the synthesis of new acetylcholine and thereby decrease the overstimulation of the cholinergic system (Kuhar and Murin 1978; Sterling et al. 1991; Sterling et al. 1993). It has also been shown that quinuclidinium derivatives are reversible inhibitors of AChE (Simeon-Rudolf et al. 1998; Reiner et al. 1999) and have protective activity against soman-poisoned mice (Radić et al. 1995;

Kovarik et al. 2015). Therefore, we focused this study on the quinuclidinium scaffold-based oximes with an aim to find more potent reactivators of both AChE and BChE. We designed and synthesized 14 quinuclidinium oximes, which differ in the size and type of the substituent at the quinuclidine nitrogen (Fig. 1). This class of compounds has the oxime group on the quinuclidinium ring, differing, in that way, from most types of reactivators studied—pyridinium or imidazolium oximes (Kovarik et al 2008b, 2019a, b; Mercey et al. 2011; Renou et al. 2013; Radić et al. 2013b; Horn et al. 2015; Winter et al. 2016; Katalinić et al. 2016; Zorbaz et al. 2018b). All compounds were tested as reactivators of VX-, tabun-, sarin-, cyclosarin- and paraoxon-inhibited AChE and BChE, as well as reversible inhibitors of these enzymes. We performed molecular docking studies to evaluate conformations of quinuclidinium oximes in the active site of human AChE and BChE, and related them to the kinetic study results. Beside this, cytotoxic profiles were evaluated on two cell lines, hepatocytes (HepG2) and neuroblastoma (SH-SY5Y), as a primary screening of compounds prior to any evaluation in vivo.

Materials and methods

Synthesis of quinuclidinium oximes

We synthesized quinuclidine 3-oxime (**Q1**) and its 13 derivatives (Fig. 1). The compound **Q1** was synthesized from quinuclidin-3-one hydrochloride (≥ 98.0%, Fluka, Honeywell Research Chemicals, Charlotte, NC, USA) following a published procedure (Sternbach and Kaiser 1952; Primožič et al. 2014). **Q2** was quaternized with methyl iodide (Lucić et al. 1997), **Q3** with allyl bromide and **Q4** with butenyl bromide (Radman Kastelic et al. 2019), **Q5** with dodecyl bromide (Skočibušić et al. 2016), **Q6** with benzyl bromide, and **Q7**–**Q14** with appropriate *meta*- and *para*-substituted benzyl bromides (Radman Kastelic et al. 2019). CHN analysis was performed for all compounds (Perkin Elmer 2400 Series II CHNS analyzer) and all compounds were found to be of > 99% purity. The synthesized quinuclidinium oximes were dissolved in water as 10 mM solution, except **Q5**, which was prepared in DMSO as a 100 mM solution.

Chemicals and enzymes

Paraoxon-ethyl (Sigma-Aldrich St. Louis, MO, USA) was prepared in ethanol, while stock solutions of sarin, cyclosarin, tabun and VX (NC Laboratory, Spiez, Switzerland) were prepared in isopropyl alcohol and further dilutions were made in water just before use. OPs were used in accordance with the safe use and safe disposition of highly toxic compounds. Acetylthiocholine (ATCh) and thiol reagent 5,5′-dithiobis(2-nitrobenzoic acid) (DTNB) were purchased from Sigma-Aldrich (St. Louis, MO, USA). MTS reagent [3-(4,5-dimethylthiazole-2-yl)-2,5-diphenyl tetrazolium bromide] for cytotoxicity assays was purchased from Promega (Madison, WI, USA).

The source of human BChE and AChE for reactivation studies was plasma and erythrocytes, respectively, obtained from heparinized blood of healthy volunteers and in accordance with the approval from the Ethics Committee of the Institute for Medical Research and Occupational Health. Erythrocytes were separated from the plasma by centrifugation, washed twice with a buffer to remove the residual plasma and diluted to the volume of the whole blood (Reiner et al. 2004; Čalić et al. 2006). For reversible inhibition studies, recombinant human AChE and purified human plasma BChE were used. These enzymes were a gift from Dr. Florian Nachon, Institut de Recherche Biomédicale des Armées, Brétigny-sur-Orge, France. According to our previous studies, no significant difference in results is expected for the same enzymes of the same human origin from two different sources (Čalić et al. 2006; Kovarik et al 2010b; Šinko et al. 2010; Zorbaz et al. 2018b).

Reversible inhibition of AChE and BChE with oximes

The enzyme activity was measured in the presence of oxime following a previously described procedure (Čalić et al. 2006; Kovarik et al. 2008a). The activity was assayed by Ellman's method (Ellman et al. 1961) where the inhibition mixture contained 0.1 M sodium phosphate buffer pH 7.4, enzyme (AChE or BChE), oxime (0.25–3 mM), DTNB (0.3 mM), and ATCh (final concentration from 0.03 to 1 mM) to start the reaction. For oxime dissolved in DMSO (**Q5**), the final DMSO concentration was kept under 0.5% to eliminate its influence on enzyme activity (Kumar and Darreh-Shori 2017; Zorbaz et al. 2018a). The measured activity in the presence of oximes was corrected for the oximolysis of ATCh (Šinko et al. 2006). The assay was performed at 25 °C in the 96-well plates on the Infinite M200PRO plate reader (Tecan Austria GmbH, Salzburg, Austria). Dissociation constants of inhibition, K_i, were determined from at least two experiments and evaluated from the effect of substrate concentration on the degree of inhibition according to the equation:

$$K_{i,\mathrm{app}} = \frac{v_i \times i}{v_0 - v_i} = K_i + \frac{K_i}{K_S} \times S \quad (1)$$

where $K_{i,\mathrm{app}}$ is the apparent enzyme-oxime dissociation constant at a given substrate concentration (S), and v_0 and v_i enzyme activities measured in the absence or in the presence of the oxime concentration (i). K_i is the enzyme-oxime dissociation constant and K_S is the enzyme–substrate

dissociation constant. The K_i values were determined from correlation $K_{i,app}$ vs. substrate concentration as described previously (Čalić et al. 2006; Kovarik et al. 2008b) using the Prism6 software (GraphPad Software, San Diego, USA).

Reactivation of OP-inhibited AChE and BChE

In the enzyme reactivation assay, plasma as the source of BChE and erythrocytes as the source of AChE were incubated with OP up to 1 h, achieving 95–100% inhibition. The inhibited enzymes were passed through a Strata C18-E column (Phenomenex, Torrance, CA, USA) prior to incubation with 1 mM oxime for the initial screening of reactivation potency at 25 °C. At specified time intervals (up to 24 h), an aliquot was taken for enzyme activity measuring upon addition of the DTNB (0.3 mM) and the substrate ATCh (1 mM final) by Ellman's method (Ellman et al. 1961). For the control sample, an equivalent amount of the uninhibited enzyme was passed through the same procedure as the reactivation mixture described above, and control activity was measured in the presence of the same oxime concentration as well. Both the activities of the control and the reactivation mixture were corrected for the oximolysis of ATCh (Šinko et al. 2006). No spontaneous reactivation was detected. Enzyme activity measurements were performed at 25 °C at 436 nm (for erythrocyte AChE) and 412 nm (for plasma BChE) on a CARY 300 spectrophotometer with a temperature controller (Varian Inc., Australia). For the most potent reactivators, detailed kinetic parameters were determined from a wider range of oxime concentrations (from 1 µM up to 5 mM).

The observed reactivation rate constant at the given oxime concentration (k_{obs}) was determined by a previously described procedure (Katalinić et al. 2016; Maček Hrvat et al. 2018). The maximal reactivation rate constant (k_{max}), phosphorylated enzyme-oxime dissociation constant (K_{OX}), the second-order rate constant of reactivation (k_r) and maximal reactivation percentage ($React_{max}$) were determined by the non-linear fit as described previously (Čalić et al. 2006).

Bioscavenging of cyclosarin in the presence of BChE and oxime Q8

Biocavenging was evaluated by following BChE activity recovery in the presence of oxime **Q8** under 10-, 50- and 100-fold excess of cyclosarin over BChE concentration. Concentration of oxime **Q8** corresponded to its BChE dissociation inhibition constant K_i (22 µM). The reaction mixture contained human plasma BChE diluted in 0.1 M phosphate buffer, DTNB, **Q8** and cyclosarin to start inhibition. After a given time, up to 4.5 h, ATCh (1 mM final) was added and residual activity was measured at 412 nm at 25 °C. The same experimental procedure was followed for progressive inhibition of BChE by cyclosarin without the presence of oxime **Q8**.

Data were expressed as BChE activity vs. time and from the initial linear part of the curve we evaluated the observed rate constant of inhibition ($k_{i,obs}$) at a given concentration of cyclosarin in the absence or presence of **Q8**. The slope presents the overall second-order rate constants of BChE inhibition and was evaluated according to a previously published procedure (Kovarik et al. 2002). Additionally, a theoretical curve was proposed to describe the complete profile of the obtained data combining two exponential equations in one: for progressive inhibition, describing the first part of the curve when a decrease in the BChE activity was dominant, and after reaching the minimum of enzyme activity, the second one for reactivation in situ to describe a part of the curve when the recovery of the enzyme activity prevailed:

$$Activity(\%) = (Y0 - \text{Plateau}) \times \left(1 + e^{-k_1 \times t} - e^{-k_2 \times t}\right) + \text{Plateau} \quad (2)$$

where $Y0$ is the maximal enzyme activity at the start, t represents a time of measurement, *Plateau* is the value of the minimal enzyme activity observed due to progressive inhibition, k_1 is the rate constant describing the initial part of the curve observed as progressive inhibition of BChE with cyclosarin in the presence of **Q8**, while k_2 is the rate constant describing the recovery part of the curve. Calculations were done using Prism6 software (GraphPad Software, San Diego, USA).

Molecular modeling

The three-dimensional structures of human AChE PDB code 4PQE (Kryger et al. 2000) and human BChE PDB code 2PM8 (Ngamelue et al. 2007) were used for molecular modeling. Oxime structures were modelled and minimized using the MMFF94 force field implemented in ChemBio3D Ultra 12.0 (PerkinElmer, Inc., Waltham, MA). Discovery Studio 2017 R2 with CDOCKER docking protocol using a CHARMm force field (BioVia, San Diego, CA, USA) generated 20 docking poses for each oxime in the active-site gorge of AChE or BChE as described earlier (Maraković et al. 2016; Zorbaz et al. 2018a). Poses were scored and ranked according to the calculated CDOCKER energy for interactions between an oxime and active site residues (i.e., hydrogen bonds, π–π interactions, cation–π interactions and electrostatic interactions). The volume of the oximes ($Å^3$) was calculated by molecular modeling software (Discovery Studio 2017 R2).

For docking studies of cyclosarin–inhibited BChE conjugate with oxime, we modified the existing crystal structure of BChE-tabun conjugate (PDB code 3DJY, Carletti et al. 2008) by replacing the (dimethylamino)(ethoxy)phosphoryl moiety with cyclohexyloxy(methyl)phosphoryl moiety

(taken from the crystal structure of *Mus musculus* AChE conjugated with cyclosarin PDB code 3ZLU, Artursson et al. 2013). The final structure of the complex was minimized using Smart Minimizer algorithm (Discovery Studio 2017 R2) with RMS gradient set to 0.005 kcal/mol·Å.

Cell lines and cytotoxicity assay

Human Caucasian hepatocyte carcinoma (HepG2, ATCC HB8065) were purchased from the American Type Culture Collection (Rockville, MD, USA) and human neuroblastoma (SH-SY5Y, ECACC 94030304) from the European Collection of Authenticated Cell Cultures (Salisbury, England, UK). HepG2 were grown in EMEM (Sigma-Aldrich, Steinheim, Germany) supplemented with 10% (v/v) fetal bovine serum (Gibco, Paisley, UK), 2 mM glutamine and 1% non-essential amino acids (NEAA, Sigma-Aldrich, Steinheim, Germany). SH-SY5Y were grown in DMEM F12 (Sigma–Aldrich, Steinheim, Germany) supplemented with 15% fetal bovine serum (Gibco, Paisley, UK), 2 mM glutamine and 1% non-essential amino acids (NEAA, Sigma-Aldrich, Steinheim, Germany). Cells were grown at 37 °C in a 5% CO_2 atmosphere. The assay was performed in 96-well with 20,000 or 40,000 cells/well. Cells were exposed to the oximes (6.25–800 µM) for 24 h. After 24 h incubation, cells were washed with PBS buffer and the cytotoxicity profile of oximes was determined measuring the succinate dehydrogenase mitochondrial activity of living cells by MTS detection reagent assay (Mosmann 1983). The procedure followed a previously described protocol (Katalinić et al. 2017) using predefined CellTiter 96® AQueous One Solution Cell Proliferation Assay (Promega, Madison, WI, USA). After 0.5–3 h the absorbance was read at 492 nm on an Infinite M200PRO plate reader (Tecan Austria GmbH, Salzburg, Austria). The total percentage of DMSO in cytotoxicity assay was 0.8% and did not influence cells. Data were evaluated from at least two or three experiments (each in duplicate or triplicate) and presented as percentage of inhibition to control untreated cells. Results were described as IC_{50} values (concentration inhibiting 50% cells) using a nonlinear fit equation predefined in Prism6 software (GraphPad Software, San Diego, USA).

Results

Synthesis of quinuclidinium oximes

The initial compound for synthesis, quinuclidin-3-one, was prepared from its commercially available hydrochloride by a previously described procedure (Grob and Renk 1954). Compound **Q1**, 3-hydroxyiminoquinuclidine was prepared by the reaction of quinuclidin-3-one with hydroxylamine hydrochloride and sodium hydroxide as described previously (Sternbach and Kaiser 1952; Primožič et al. 2014). To prepare compounds **Q2**–**Q14** (Fig. 1), the Menshutkin reaction was employed to convert tertiary amine to quaternary ammonium salt by the reaction with the appropriate alkyl/aryl halide as described previously (Lucić et al. 1997; Skočibušić et al. 2016; Radman Kastelic et al. 2019). Products were obtained in 60−90% yield and all of them were solids that precipitated using diethyl ether. All compounds had an (*E*)-configuration of the oxime group which is expected to be thermodynamically favored (Skočibušić et al. 2016).

Reversible inhibition of AChE and BChE with oximes

All of the tested quinuclidinium oximes (**Q1**−**Q14**) reversibly inhibited the activity of AChE and BChE. The determined dissociation constants K_i and *in silico* calculated molecular volume *V* are given in Table 1. Both cholinesterases exhibited the lowest binding affinity for 3-hydroxyiminoquinuclidine (**Q1**). The quaternization of the nitrogen atom of the quinuclidine moiety with the aliphatic chain, or the benzyl group even more, improved the affinity for oxime binding compared to **Q1**. The highest affinity of both cholinesterases was observed for **Q5** with a dodecyl aliphatic chain attached to the quinuclidinium ring and the largest molecule in the set (341 $Å^3$). Furthermore, the AChE binding affinity varied by the substituent on the benzene ring $–NO_2 > –CH_3 \geq –Br > –Cl$ favoring its *meta* position. The highest five-fold *meta* to *para* ratio was observed for **Q11** and **Q12** with the methyl substituent. Although the BChE affinity was not affected as much by substituents, an opposite preference to AChE (*para* to *meta*) was observed. In terms of the binding selectivity and K_i AChE/K_i BChE ratio, the maximal difference, about three, was shown for **Q8** and **Q12**.

Molecular modeling of AChE and BChE in complex with quinuclidinium oximes

Molecular modeling of AChE or BChE in complex with quinuclidinium oximes indicated that oximes bind in a similar manner to both active sites. The quinuclidinium moiety interacts with residues of the choline-binding site and forms hydrogen bonds with the catalytic triad residues. The rest of the oxime molecule faces towards the gorge entrance and interacts with the residues of the periphery. **Q5**, the oxime with the highest inhibition potency, forms in AChE additional alkyl-π interactions with aromatic residues Trp86 of the choline binding site and Trp286 of the peripheral site, electrostatic interaction with Trp86 and hydrogen bond with Tyr133 (Fig. 2a). In BChE this oxime shows additional cation-π interactions with residue Trp82 of the choline binding site, hydrogen

Table 1 Reversible inhibition of AChE and BChE by quinuclidinium oximes and their calculated molecular volume

Oxime	– *R*	AChE K_i (μM)	BChE K_i (μM)	K_i AChE/K_i BChE	*V* (Å^3)
Q1	–	3800 ± 450	2400 ± 290	1.6	136.8
Q2	$–CH_3$	750 ± 210	880 ± 140	0.9	156.8
Q3	$–C_3H_5$	520 ± 140	770 ± 140	0.7	185.4
Q4	$–C_4H_7$	550 ± 220	190 ± 40	2.9	202.3
Q5	$–C_{12}H_{25}$	6 ± 1	4 ± 1	1.7	341.0
Q6	$–CH_2$-Ph	160 ± 8	190 ± 20	0.9	230.8
Q7	$–CH_2$-Ph-*m*-Br	32 ± 2	39 ± 7	0.8	250.6
Q8	$–CH_2$-Ph-*p*-Br	67 ± 14	22 ± 1	3.1	250.7
Q9	$–CH_2$-Ph-*m*-Cl	41 ± 2	72 ± 11	0.6	246.2
Q10	$–CH_2$-Ph-*p*-Cl	91 ± 18	62 ± 5	1.5	246.2
Q11	$–CH_2$-Ph-*m*-CH_3	27 ± 2	41 ± 6	0.7	247.4
Q12	$–CH_2$-Ph-*p*-CH_3	136 ± 6	42 ± 6	3.3	247.4
Q13	$–CH_2$-Ph-*m*-NO_2	18 ± 1	25 ± 2	0.7	256.9
Q14	$–CH_2$-Ph-*p*-NO_2	49 ± 3	20 ± 2	2.5	257.0

Dissociation inhibition constants (K_i ± standard error) were determined from at least three experiments

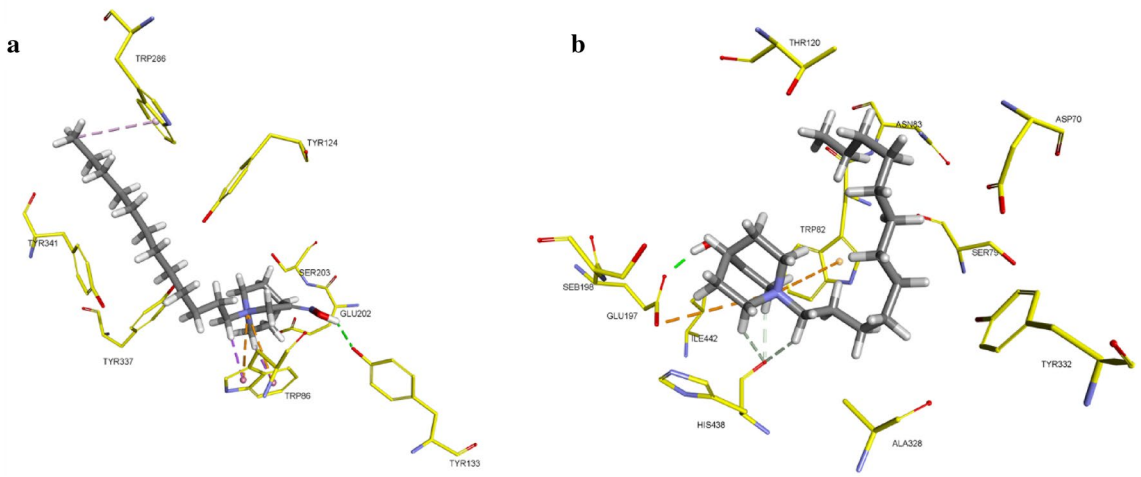

Fig. 2 Orientation of oxime **Q5** (grey) in the active site of **a** AChE (from PDB code 4PQE, Kryger et al. 2000) and **b** BChE (from PDB code 2PM8, Ngamelue et al. 2007). Protein residues carbon atoms are shown in yellow, oxygen in red and nitrogen in blue. Hydrogen bonds are shown in green and light green dashed lines, electrostatic interactions in orange and alkyl–π interactions in light purple dashed lines (color figure online)

bonds with Glu197 and the catalytic triad residue His438, and electrostatic interactions with Glu197 (Fig. 2b).

Molecular modeling of AChE and benzyl group derivatives **Q7**−**Q14** revealed that the oxime *meta* and *para* substituent pairs overlap and can adopt almost the same orientation in the active site as shown in Fig. 3. In other words, there is no significant difference in positioning of analogue pairs of oximes in the AChE active site that could explain the *meta*-over *para*-preference.

Screening of oxime-assisted reactivation of human AChE and BChE inhibited by OPs

An initial reactivation screening potency to reactivate AChE and BChE inhibited by sarin, cyclosarin, VX, tabun and paraoxon was evaluated at the given concentration of an oxime. Obtained results in terms of the observed first-order reactivation rate constant (k_{obs}) achieved by 1 mM oxime are presented in Fig. 4a for AChE and Fig. 4b for BChE.

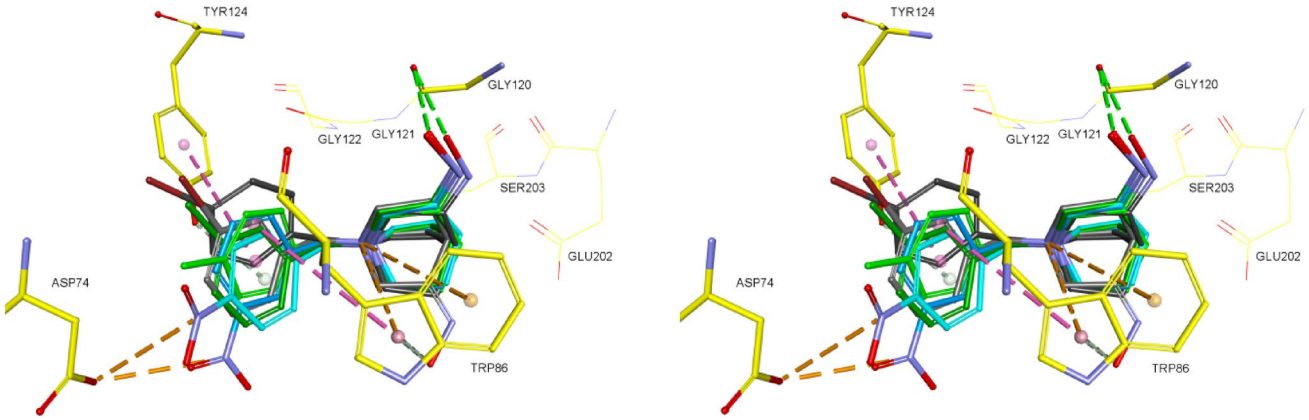

Fig. 3 Stereo view of oxime pairs **Q7** and **Q8** (dark grey), **Q11** and **Q12** (green) and **Q13** and **Q14** (light blue) inside the active gorge of AChE (model from PDB code 4PQE, Kryger et al. 2000; wire-frame and sticks) after superposition. Protein residue carbon atoms are shown in yellow, oxygen in red and nitrogen in blue. Hydrogen bonds are shown in green dashed lines, electrostatic interactions in orange dashed lines, π–π interaction in pink and cation–π interaction in brown dashed lines (color figure online)

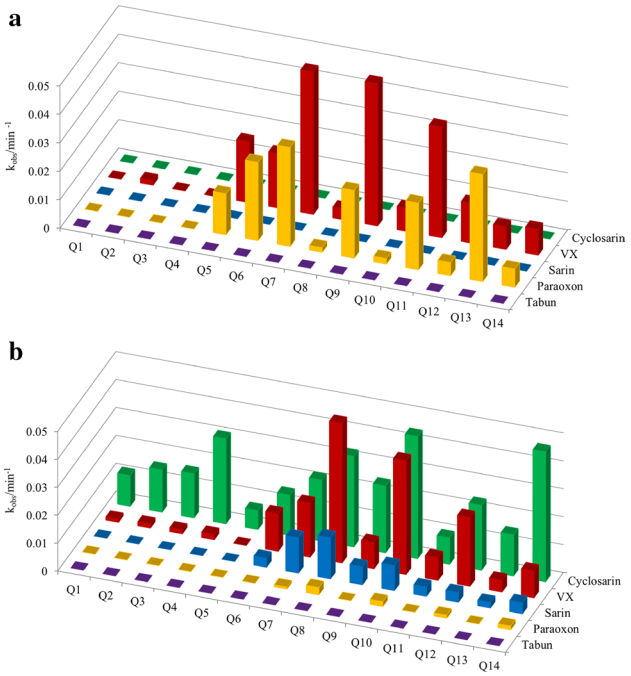

Fig. 4 Observed first-order rate constants of reactivation (k_{obs}) of OP-inhibited **a** human erythrocyte AChE; **b** human plasma BChE, by 1 mM oximes recorded within 24 h. Constants present the mean of at least two experiments with the standard error less than 10%

Ten of tested oximes (**Q5**−**Q14**) were able to reactivate VX- and paraoxon-inhibited AChE reaching the maximal reactivation percentage from 50−100% in 24 h. The reactivation screening profile for these OP indicated that quinuclidinium oximes with meta-substituents at the benzyl group were more efficient reactivators than their *para*-analogues. The highest reactivation rates for AChE inhibited by VX of 0.05 min^{-1} were observed in the case of **Q7** (*m*-Br) and **Q9** (*m*-Cl), where the reactivation maximum of 90% was achieved within 1 h or 1.5 h, respectively (Fig. 4a). The highest reactivation rates for AChE inhibited by paraoxon of 0.035 min^{-1} were observed with **Q7** (*m*-Br) and **Q13** (*m*-NO_2), where the reactivation maximum of 80% was achieved within 2 h (Fig. 4a). Unfortunately, for sarin, cyclosarin and tabun none of the oximes showed any favorable result reaching less than 20% of AChE reactivation within 24 h.

In the case of BChE, quinuclidinium oximes at 1 mM concentration reactivated its conjugates with sarin, cyclosarin and VX, but not with paraoxon and tabun (Fig. 4b). In general, the observed reactivation rate constants for sarin-, cyclosarin- and VX-inhibited BChE were higher for oximes with *para*-substituents on the benzyl group compared to their *meta*-analogues. However, reactivation of VX-inhibited BChE by oxime **Q8**−**Q14** reached plateau of 40% after only a few hours. Sarin-inhibited BChE was reactivated 80–95% in 4–24 h by quinuclidinium oximes having a benzyl group (**Q6**−**Q14**). Cyclosarin-inhibited BChE was the most inclined to reactivation by all studied oximes achieving the reactivation maximum of 90% within 60−90 min with oximes **Q8** (*p*-Br), **Q10** (*p*-Cl) and **Q14** (*p*-NO_2).

Detailed reactivation kinetics with selected oximes

For oximes that reactivated OP-inhibited AChE or BChE up to 90% within 30 min to 4 h, a wider concentration range (from 1 µM up to 5 mM) was used for evaluation of reactivation kinetics and determination of reactivation rate constants.

In the case of AChE, those selection criteria sorted three and six oximes for reactivation of VX and paraoxon conjugates, respectively (Table 2). The reactivation of VX-inhibited AChE with oximes **Q7**, **Q9** and **Q11**, reached maximal 90–100% in a short time with relatively high k_{max} values.

Table 2 Reactivation of VX and paraoxon-inhibited human erythrocyte AChE with selected quinuclidinium oximes and HI-6

OP	Oxime	k_{max} (min^{-1})	K_{OX} (mM)	k_r (M^{-1} min^{-1})	$React_{max}$ (%)	t (min)
VX	**Q7**[a]	–	–	44 ± 2	95	60
	Q9	0.12 ± 0.02	3.0 ± 0.9	40 ± 6	100	60
	Q11	0.23 ± 0.04	5.2 ± 1.4	43 ± 4	90	120
	HI-6[b]	0.33 ± 0.02	0.06 ± 0.01	5740 ± 1120	90	15
Paraoxon	**Q5**[a]	–	–	17 ± 0.3	90	240
	Q6	0.136 ± 0.008	3.0 ± 0.3	46 ± 2	95	120
	Q7[a]	–	–	51 ± 2	95	120
	Q9[a]	–	–	42 ± 1	100	120
	Q11[a]	–	–	28 ± 1	95	120
	Q13[a]	–	–	32 ± 2	100	150
	HI-6[b]	0.026 ± 0.001	0.59 ± 0.05	50 ± 2	90	170

The kinetic parameters (± standard error): first-order reactivation rate constant (k_{max}), phosphylated enzyme-oxime dissociation constant (K_{OX}), the second-order reactivation rate constant (k_r), reactivation maximum ($React_{max}$) and time of reaching the reactivation maximum (t) were determined from at least three experiments

[a]Due to a linear dependence of k_{obs} vs. oxime concentration, k_{max} and K_{OX} could not be determined

[b]Zorbaz et al. 2018a

However, due to a low binding affinity, i.e., high K_{OX}, the overall reactivation rate k_r was only about 40 M^{-1} min^{-1} (Table 2), about 100-fold lower than for HI-6.

Selected oximes, **Q5**, **Q6**, **Q7**, **Q9**, **Q13** and **Q11**, enabled the completion of reactivation of AChE inhibited by paraoxon within 2−4 h. However, in the case of VX, as a consequence of low binding affinity the overall reactivation efficiency was poor (Table 2). Moreover, all of the tested oximes, except **Q6**, probably due to low binding affinity of conjugated AChE, exhibited a linear dependence of k_{obs} vs. oxime concentration in the studied concentration range, and we were not able to evaluate intrinsic reactivation constants (k_{max} and K_{OX} constants).

In the case of BChE, the chosen criteria of reactivation up to 90% within 30 min to 4 h singled out quinuclidinium oximes **Q8** and **Q10** for detailed analysis of its VX- and **Q4**, **Q8**, **Q10** and **Q14** for its cyclosarin conjugates reactivation. The determined reactivation constants are given in Table 3. The reactivation of VX-inhibited BChE with both **Q8** and **Q10** reached a plateau at 40% of maximal reactivation in only an hour (as observed in the screening as well). The cyclosarin-BChE conjugate was efficiently reactivated by all selected oximes approaching 90% of restored BChE activity within 1 h. The highest overall cyclosarin-reactivation rate of 19,670 M^{-1} min^{-1} was achieved by **Q8**, an oxime with the bromo-benzyl substituent at the quinuclidinium moiety. This remarkable result was primarily a consequence of the highest binding affinity, 3.1 µM. It is worth noting that the affinity of cyclosarin-BChE conjugate spanned three orders of magnitude for selected oximes showing a significant dependence on the substituents present at the benzyl ring: -Br ≥ -Cl > -NO_2 > -butyl.

Table 3 Reactivation of VX and cyclosarin-inhibited human plasma BChE with selected quinuclidinium oximes and HI-6

OP	Oxime	k_{max} (min^{-1})	K_{OX} (µM)	k_r (M^{-1} min^{-1})	$React_{max}$ (%)	t (min)
VX	**Q8**	0.026 ± 0.002	42 ± 9	612 ± 125	40	60
	Q10	0.027 ± 0.001	137 ± 17	263 ± 85	40	60
	HI-6[a]	0.12 ± 0.03	370 ± 230	330 ± 230	85	120
Cyclosarin	**Q4**	0.094 ± 0.007	1150 ± 180	82 ± 7	90	60
	Q8	0.061 ± 0.001	3.1 ± 0.3	19670 ± 1873	85	40
	Q10	0.039 ± 0.001	10 ± 2	3387 ± 530	85	60
	Q14	0.090 ± 0.004	360 ± 50	249 ± 26	90	60
	HI-6[a]	–	–	780 ± 30	90	30

The kinetic parameters (± standard error): first-order reactivation rate constant (k_{max}), phosphylated enzyme-oxime dissociation constant (K_{OX}), the second-order reactivation rate constant (k_r), reactivation maximum ($React_{max}$) and time of reaching the reactivation maximum (t) were determined from at least two experiments

[a]Zorbaz et al. 2018a

Molecular modeling of cyclosarin-phosphonylated BChE in complex with oxime Q8

Modeling of the complex between **Q8** and cyclohexyloxy(methyl)phosphoryl-BChE conjugate clarified the possible interactions that may lead to its outstanding reactivation efficiency. The position of **Q8** in the active site of BChE, given in Fig. 5, showed two key features. The first one is related to its bromo-benzyl group moiety interactions with the choline binding site residue Trp82. The second key feature is favorable orientation of the quinuclidinium ring and the bromophenyl moiety of **Q8**, directed by the position of the cyclohexyl moiety conjugated with the active site serine. This causes an additional stabilization of **Q8** that gives the advantage to the oxime group for a nucleophilic attack on the phosphorus atom at a distance of about 6.27 Å.

Biocavenging of cyclosarin by BChE and oxime Q8

Bioscavenging of cyclosarin was proven in assays where up to 100-fold excess of cyclosarin over BChE concentration was successfully decomposed by the oxime-assisted reactivation as it is given in Fig. 6. The activity of BChE was recovered when cyclosarin was exhausted. As results indicated, the BChE-**Q8** pair had the capacity to decompose up to 15 nM cyclosarin within 2–3 h. The initial part of the activity curves was marked by the progressive inhibition of BChE with cyclosarin that resulted in a minimum of the BChE activity. In the presence of **Q8**, besides of a four-fold decrease of the overall inhibition rate (Fig. 6d), the minimum of the activity was never less than 20%. In other words, along with two effects of oxime **Q8** presence in the mixture—reversible binding to uninhibited and fast reactivation of inhibited enzyme, it preserved BChE activity from being completely nullified. After only 5–15 min, cyclosarin concentration decreased to the point where progressive inhibition was being overcome by the **Q8**-assisted BChE reactivation that lead to fully restored BChE activity. This effect was particularly pronounced at low cyclosarin concentration (1.5 nM) where BChE activity recovery was observed early on after 10–15 min (Fig. 6a). Moreover, in either of the experiments there is no BChE reinhibition within 4 h as a result of full decomposition of cyclosarin by the BChE-**Q8** pair, and on the other side this could be a proof that the product of bioscavenging, phosphonylated-oxime, is not stable and its inhibition potency is neglectable. In addition, we were able to describe the experimental data by the proposed theoretical curve (Fig. 6), and the obtained rate constants given in Table 4. The relatively high coefficient of determination R^2 of 0.78–0.90 demonstrates that two evaluated reactions (progressive inhibition and reactivation) follow known kinetics that could be used for bioscavenging effects as well as evaluation of the relevant kinetic constants. However, some discrepancies with experimental points were observed especially for bioscavenging of the highest cyclosarin concentration (Fig. 6c) probably due to the limitations of the proposed equation that places more focus on the data points obtained at the start. In addition, an additional kinetics of cyclosarin concentration change in time, that was not taken here into account, could change the fit agreement.

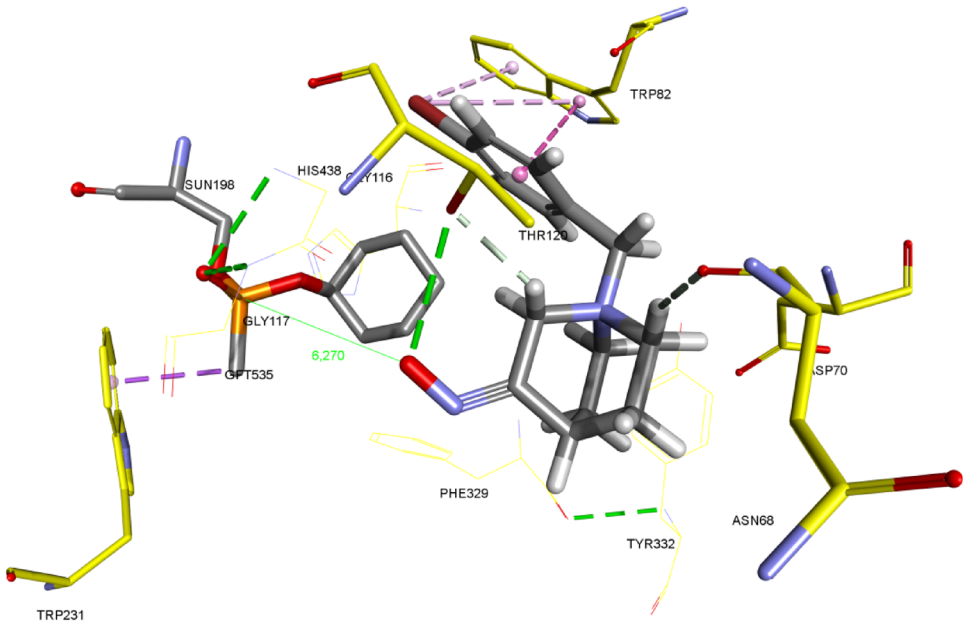

Fig. 5 Molecular modeling of interactions between **Q8** oxime and *in silico* model of human cyclosarin-inhibited BChE. The model of human cyclosarin-inhibited BChE was made using crystal structures of tabun-inhibited BChE (PDB code 3DJY, Carletti et al. 2008) and cyclosarin-inhibited AChE (PDB code 3ZLU, Artursson et al. 2013). Protein residue carbon atoms are shown in yellow, oxygen in red and nitrogen in blue. Hydrogen bonds are shown in green and light green dashed lines and π–π interaction in pink dashed lines (color figure online)

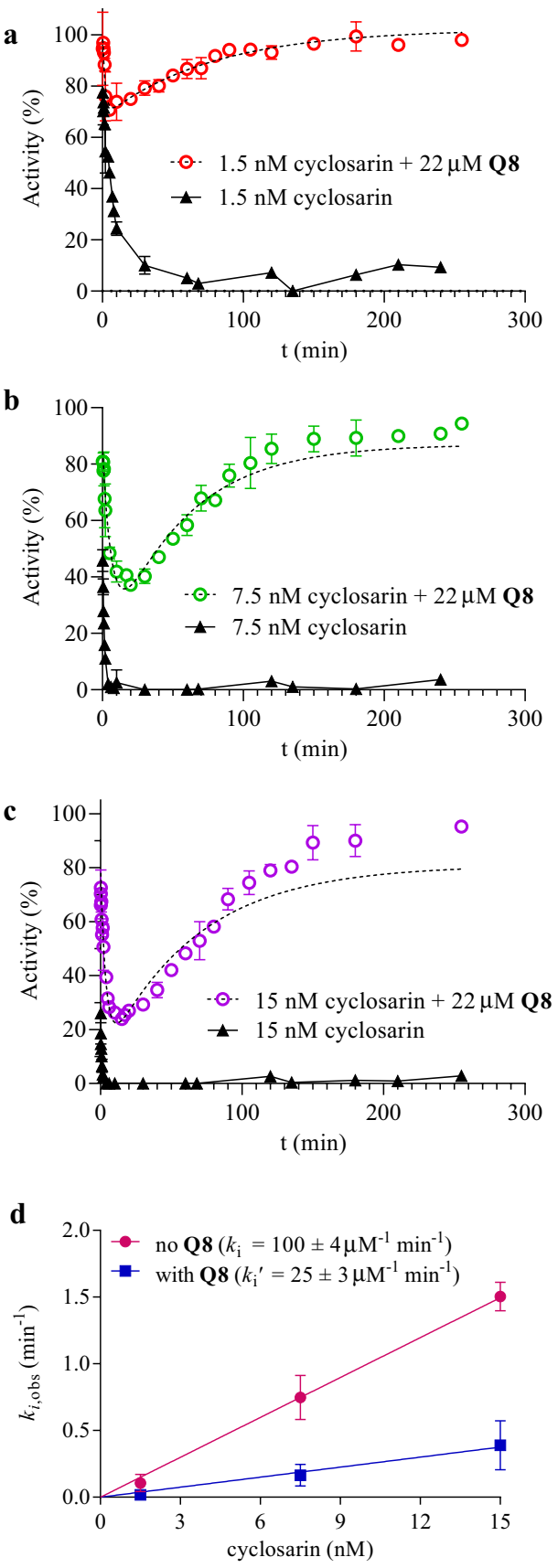

Fig. 6 The effect of the presence of oxime **Q8** on progressive inhibition of BChE by cyclosarin that resulted with bioscavenging of cyclosarin with BChE and oxime **Q8** in **a** 10-, **b** 50- and **c** 100-fold excess of cyclosarin over the BChE concentration. Experimental data presents the enzyme activity and mean of at least three measurements. The dotted lines represent a theoretical curve obtained with Eq. 2 **d** evaluation of the overall inhibition rate constant of BChE by cyclosarin in the absence (k_i) or presence of **Q8** (k_i'), equivalent to the slope of each line

Cytotoxicity of quinuclidinium oximes

Cytotoxicity of quinuclidinium oximes was evaluated on SH-SY5Y and HepG2 cell lines in the concentration range from 6–800 µM. As Fig. 7 demonstrates, only oxime **Q5** showed a significant cytotoxic profile, with IC_{50} values of 220 ± 5 µM for SH-SY5Y and 25 ± 4 µM for HepG2. The other oximes were not toxic in the applied concentration range to either of the cell line tested.

Discussion

We can generally emphasize that all herein tested quinuclidinium oximes bind to both cholinesterases in a reversible inhibitor manner. The presence of the benzyl moiety attached to the quinuclidinium quaternary core proved important for potent binding to both active sites confirming also previous studies (Simeon-Rudolf et al. 1998; Bosak et al. 2005; Odžak et al. 2007a; Primožič et al. 2012). The observed similarities of the tested oximes in cholinesterase inhibition potency are most probably a consequence of the interactions with conserved aromatic residues, rich in π electrons, in the active site of AChE and BChE (Kryger et al. 2000), as indicated by molecular modeling. Furthermore, their dissociation constants were in the same range as the ones of pyridinium oximes studied nowadays as efficient reactivators (Odžak et al. 2007b; Kovarik et al. 2007, 2008a; Katalinić et al. 2017; Zorbaz et al. 2018a). Additionally, the spatial constraints within the AChE active site distinguished the positioning by the substituent on the aromatic ring, favoring thereby *meta* over their *para* analogs. Interestingly, the most potent inhibitor of both enzymes was oxime **Q5** with a long aliphatic chain attached to the quinuclidinium quaternary moiety. This shows that complex alkyl chains could compete with aromatic rings as the moiety of choice in structural design of cholinesterase inhibitors. On the other hand, hydrophobic moiety of **Q5** could be the cause of its observed citotoxicity, by possible formation of micelles that such compounds can form and by which they affect cell membranes (Singh et al. 2013; Mukherjee et al. 2014). However, one should be aware that a non-cytotoxic effect on cells still does not mean that other quinuclidinium oximes would have an acceptable profile in vivo since the

Table 4 Kinetic parameters describing the theoretical curves for scavenging of cyclosarin by BChE and oxime **Q8** (22 µM) by applying Eq. 2 (parameters ± standard error)

Cyclosarin (nM)	R^2	*Y*0 (%)	k_1 (min^{-1})	*Plateau* (%)	k_2 (min^{-1})	*Y*min (%)	*Y*max (%)	Time (h)
1.5	0.78	100 ± 30	0.52 ± 0.14	68 ± 3	0.0130 ± 0.003	72	100	2
7.5	0.90	87 ± 3	0.15 ± 0.028	8 ± 9	0.0190 ± 0.003	36	86	2.5
15	0.89	81 ± 3	0.26 ± 0.039	7 ± 4	0.0155 ± 0.002	22	80	3

Cyclosarin was in 10-, 50- and 100-fold excess over BChE concentration

**Y*0—the maximal BChE activity at the start; *Plateau*—the minimal enzyme activity observed by progressive inhibition of BChE with cyclosarin; k_1—the rate constant describing the first part of the curve observed as progressive inhibition with cyclosarin in the presence of Q8; k_2—the rate constant describing the second part of the curve observed as reactivation of BChE activity; *Y*min, *Y*max—minimal and maximal BChE activity observed in the experiment

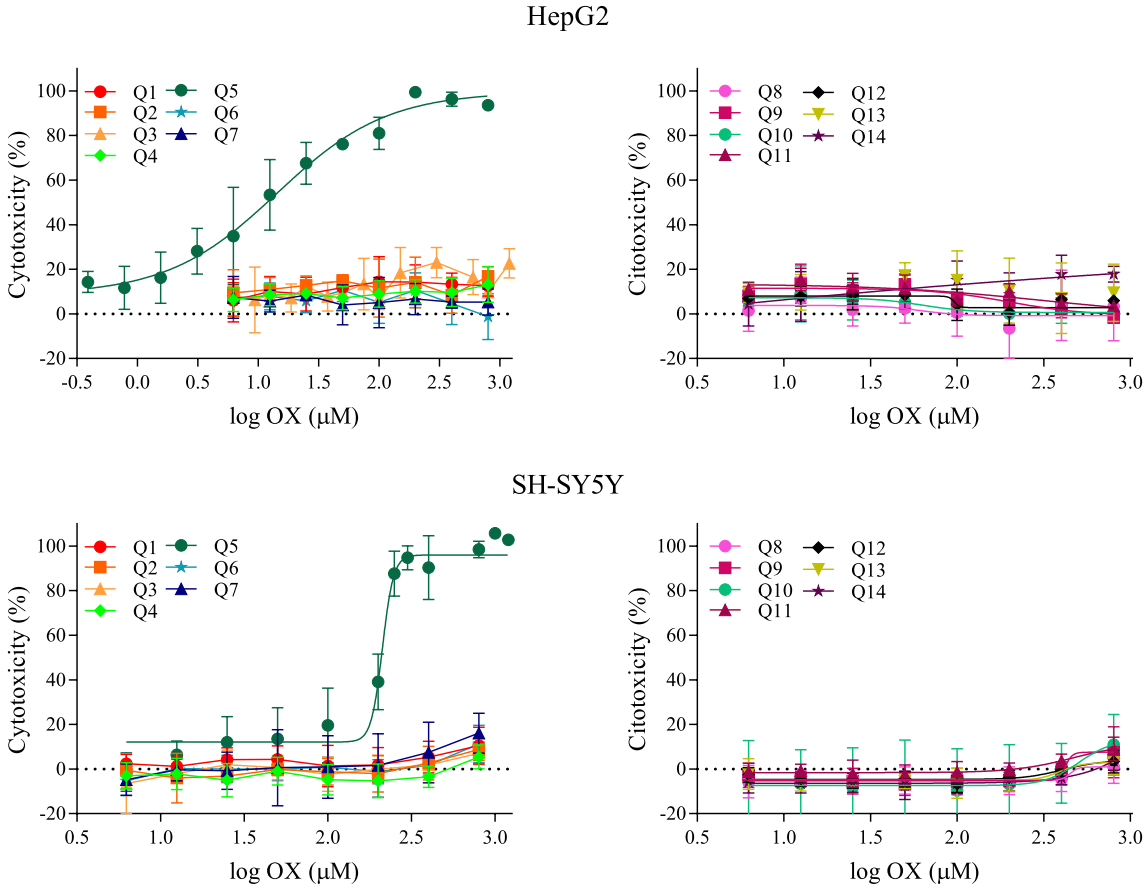

Fig. 7 The cytotoxicity of the tested oximes in the HepG2 and SH-SY5Y cell line. The experimental data presents a mean of at least three experiments

mechanism underlining toxicities on these two systems differs (Wilkening et al. 2003; Čalić et al. 2006; Kovarik et al. 2019a, c). Namely, their toxicity in vivo could still be induced by their inhibitory properties on AChE or other toxic mechanism (Estevan et al. 2013).

The reactivation efficiency of quinuclidinium oximes was tested for AChE and BChE inhibited by VX, sarin, cyclosarin, tabun and paraoxon. Results showed that phosphylated AChE was quite resistant to reactivation by quinuclidinium oximes. Reactivation was observed only for VX- and paraoxon-inhibited AChE, but only with oximes with more complex substituents i.e., **Q5**-**Q14**, favoring among them *meta*-positioned analogues just as it was determined in the reversible inhibition studies. However, their reactivation efficiency for AChE was not better than that of standard oximes like obidoxime, HI-6 and Hlö-7 (Worek et al. 1998; Zorbaz et al. 2018a) or other oximes marked as leading experimental antidotes from recent studies (Mercey et al. 2011; Renou

et al. 2013; Radić et al. 2013b; Winter et al. 2016; Sit et al. 2018; Zorbaz et al. 2018b; Kovarik et al. 2019a). OP-inhibited BChE was more susceptible to reactivation, and similarly to AChE, quinuclidinium oximes with benzyl moiety were more efficient in restoring BChE activity. Oppositely to AChE, oximes with *para*-substituents on the benzyl group were more efficient in reactivation of BChE. Their highest efficiency was observed for reactivation of BChE inhibited by VX and cyclosarin. The obtained constants for VX-inhibited BChE reactivation placed these oximes in line with several 3-hydroxy-2-pyridine aldoximes previously described as potent BChE reactivators (Zorbaz et al. 2018a), but at the same time, they were less efficient than, for example, the pyridinium or imidazolium class of oximes (Sit et al. 2014; Horn et al. 2015; Katalinić et al. 2016; Kovarik et al. 2019b). However, the notable efficiency of quinuclidinium oximes for VX-inhibited BChE stopped at a maximum of only 40%. A background for the occurrence of such plateaus is unclear, but a similar observation in the reactivation of BChE inhibited by the various OP was reported in other studies as well (Kovarik et al. 2010a; Katalinić et al. 2018).

For cyclosarin-inhibited BChE, the most exceptional result was achieved by oxime **Q8** that had an overall reactivation rate constant of almost 20,000 M^{-1} min^{-1}. Such a reactivation potency is even more significant when we compare it to standard reactivator HI-6 or other pyridinium or imidazolium oximes described previously as potent reactivators of BChE (Kovarik et al. 2004, 2006, 2008b; Horn et al. 2015; Katalinić et al. 2016; Zorbaz et al. 2018a, 2019). The main reason for its efficiency seems to be related to a high K_i vs. K_{OX} ratio, which means that phosphonylated BChE had seven times higher affinity for this oxime than non-phosphonylated BChE. If compared to other quinuclidinium analogues tested here, it seems that the presence of the *para*-positioned bromo-substituent on the phenyl ring played a crucial role for such affinity. According to molecular modeling results, the other relevant moment seems to be steric constrain formed by the conformation of the cyclohexyl conjugate at the catalytic serine of BChE that enables specific molecular interactions of the quinuclidinium ring and the bromophenyl group of **Q8** with active site residues in a favorable position for reactivation.

Furthermore, oxime **Q8** as the most favourable oxime according to the determined constants K_i, K_{OX}, and k_r were tested in combination with BChE for the bioscavenging of cyclosarin, since such a pair could be considered as a pseudo-catalytic system capable of OP degradation in poisoning treatment (Saxena et al. 2006; Masson and Lockridge 2010; Kovarik et al. 2015; Masson and Nachon 2017). The efficiency of **Q8** in BChE reactivation was verified once more, and as a result, we observed a high decomposition rate of up to 100-fold higher cyclosarin concentration over the enzyme. In other words, the negative effect of cyclosarin as a fast-acting progressive inhibitor was attenuated within 2 h by the oxime **Q8**-assisted ongoing reactivation of BChE. To our knowledge, this is the most significant result of BChE-based cyclosarin scavenging described so far. Moreover, full BChE activity recovery, and the stability of activity over time, indicates that there was no subsequent reinhibition of the BChE by phosphonylated oxime formed during reactivation and more importantly, cyclosarin seems to be totally decomposed. However, the observed cyclosarin decomposition should be confirmed by chemical analysis as well. Lastly, the fact that **Q8** will surely protect AChE from cyclosarin inhibition due to reversible binding and that the inhibition of BChE by cyclosarin is about two times faster than that of AChE (Aurbek et al. 2009), contribute to the results we obtained for enzyme-oxime pair and additionally underline the significance of our study.

Conclusions

We evaluated 14 structural analogues of quinuclidinium oximes as potential antidotes for OP poisoning treatment. The reactivation efficiency strongly depended on the conjugated OP and the structure of the oxime. Furthermore, only oximes with benzyl group attached to the quinuclidinium core were reactivating both cholinesterases efficiently. Oximes with *meta*-substituent on the benzyl were more efficient for OP-inhibited AChE, while oximes with *para*-substituents were more efficient for OP-inhibited BChE. This stresses the complexity of the reactivation process, shows how it is governed by many factors and that finding a potential universal antidote against a range of OPs, equally effective for both cholinesterases is still a great challenge. Out of all 14 quinuclidinium oximes, oxime **Q8** (*p*-Br) had the highest determined overall reactivation rate of approximately 20,000 M^{-1} min^{-1} for cyclosarin-inhibited BChE. Due to the efficient reactivation, oxime **Q8** in combination with BChE exhibited a capability to act as a bioscavenger of cyclosarin, and as non-cytotoxic compound it presents a scaffold for the future development of BChE-based bioscavengers.

Acknowledgements We are grateful to Makso Herman for language editing. We also thank Dr Chistopher Curty for a helpful assistance with purchasing organophosphorus compounds, and Dr Florian Nachon for providing the human recombinant AChE and human purified BChE.

Author contributions IP designed and ARK and IP synthesized the oximes; MK, GŠ and ZK conceived and designed the experiments; AZ performed experiments and analyzed the data; GŠ performed computational molecular modeling; AZ, MK, GŠ, IP and ZK contributed to writing the paper. All authors have read the manuscript and approved its submission.

Funding This study was supported by the Croatian Science Foundation (IP-2018-01-7683 to ZK, UIP-2017-05-7260 to MK and IP-2016-06-3775 to IP).

Compliance with ethical standards

Conflict of interest The authors declare no conflict of interest.

References

Artursson E, Andersson PO, Akfur C, Linusson A, Börjegren S, Ekström F (2013) Catalytic-site conformational equilibrium in nerve-agent adducts of acetylcholinesterase: possible implications for the HI-6 antidote substrate specificity. Biochem Pharmacol 85(9):1389–1397. https://doi.org/10.1016/j.bcp.2013.01.016

Ashani Y, Leader H, Aggarwal N, Silman I, Worek F, Sussman JL, Goldsmith M (2016) *In vitro* evaluation of the catalytic activity of paraoxonases and phosphotriesterases predicts the enzyme circulatory levels required for in vivo protection against organophosphate intoxications. Chem Biol Interact 259(Pt B):252–256. https://doi.org/10.1016/j.cbi.2016.04.039

Aurbek N, Thiermann H, Eyer F, Eyer P, Worek F (2009) Suitability of human butyrylcholinesterase as therapeutic marker and pseudo catalytic scavenger in organophosphate poisoning: a kinetic analysis. Toxicology 259(3):133–139. https://doi.org/10.1016/j.tox.2009.02.014

Bosak A, Primožič I, Oršulić M, Tomić S, Simeon-Rudolf V (2005) Enantiomers of quinuclidin-3-ol derivatives: resolution and interactions with human cholinesterases. Croat Chem Acta 78:121–128

Čalić M, Lucić Vrdoljak A, Radić B, Jelić D, Jun D, Kuča K, Kovarik Z (2006) In vitro and in vivo evaluation of pyridinium oximes: mode of interaction with acetylcholinesterase, effect on tabun- and soman-poisoned mice and their cytotoxicity. Toxicology 219:85–96. https://doi.org/10.1016/j.tox.2005.11.003

Čalić M, Bosak A, Kuča K, Kovarik Z (2008) Interactions of butane, but-2-ene or xylene-like linked bispyridinium para-aldoximes with native and tabun-inhibited human cholinesterases. Chem Biol Interact 175(1–3):305–308. https://doi.org/10.1016/j.cbi.2008.04.010

Carletti E, Li H, Li B, Ekström F, Nicolet Y, Loiodice M, Gillon E, Froment MT, Lockridge O, Schopfer LM, Masson P, Nachon F (2008) Aging of cholinesterases phosphylated by tabun proceeds through *O*-dealkylation. J Am Chem Soc 130(47):16011–16020. https://doi.org/10.1021/ja804941z

Dolgin E (2013) Syrian gas attack reinforces need for better anti-sarin drugs. Nat Med 19:1194–1195. https://doi.org/10.1038/nm1013-1194

Eddleston M (2019) Novel clinical toxicology and pharmacology of organophosphorus insecticide self-poisoning. Annu Rev Pharmacol Toxicol 59:341–360. https://doi.org/10.1146/annurev-pharmtox-010818-021842

Ellman GL, Courtney KD, Andres V Jr, Featherstone RM (1961) New and rapid colorimetric determination of acetylcholinesterase activity. Biochem Pharmacol 7:88–95. https://doi.org/10.1016/0006-2952(61)90145-9

Estevan C, Vilanova E, Sogorb AS (2013) Chlorpyrifos and its metabolites alter gene expression at non-cytotoxic concentrations in D3 mouse embryonic stem cells under in vitro differentiation: Considerations for embryotoxic risk assessment. Tox Lett 217:14–22. https://doi.org/10.1016/toxlet.2012.11.026

Grob CA, Renk E (1954) 3-Chinuclidincarbonsaure. Helv Chim Acta 37:1689–1698

Gunnell D, Knipe D, Chang SS, Pearson M, Konradsen F, Lee WJ, Eddleston M (2017) Prevention of suicide with regulations aimed at restricting access to highly hazardous pesticides: a systematic review of the international evidence. Lancet Glob Health 5(10):e1026–e1037. https://doi.org/10.1016/S2214-109X(17)30299-1

Gupta RD, Goldsmith M, Ashani Y, Simo Y, Mullokandov G, Bar H, Ben-David M, Leader H, Margalit R, Silman I, Sussman JL, Tawfik DS (2011) Directed evolution of hydrolases for prevention of G-type nerve agent intoxication. Nat Chem Biol 7(2):120–125. https://doi.org/10.1038/nchembio.510

Horn G, Wille T, Musilek K, Kuča K, Thiermann H, Worek F (2015) Reactivation kinetics of 31 structurally different bispyridinium oximes with organophosphate-inhibited human butyrylcholinesterase. Arch Toxicol 89(3):405–414. https://doi.org/10.1007/s00204-014-1288-5

Hulse EJ, Haslam JD, Emmett SR, Woolley T (2019) Organophosphorus nerve agent poisoning: managing the poisoned patient. Br J Anaesth 123(4):457–463. https://doi.org/10.1016/j.bja.2019.04.061

Katalinić M, Maček Hrvat N, Baumann K, Morasi Piperčić S, Makarić S, Tomić S, Jović O, Hrenar T, Miličević A, Jelić D, Žunec S, Primožič I, Kovarik Z (2016) A comprehensive evaluation of novel oximes in creation of butyrylcholinesterase-based nerve agent bioscavengers. Toxicol Appl Pharmacol 310:195–204. https://doi.org/10.1016/j.taap.2016.09.015

Katalinić M, Zandona A, Ramić A, Zorbaz T, Primožič I, Kovarik Z (2017) New Cinchona oximes evaluated as reactivators of acetylcholinesterase and butyrylcholinesterase inhibited by organophosphorus compounds. Molecules 22:1–13. https://doi.org/10.3390/molecules22071234

Katalinić M, Šinko G, Maček Hrvat N, Zorbaz T, Bosak A, Kovarik Z (2018) Oxime-assisted reactivation of tabun-inhibited acetylcholinesterase analysed by active site mutations. Toxicology 406–407:104–113. https://doi.org/10.1016/j.tox.2018.05.008

Kovarik Z, Latas T, Simeon-Rudolf V (2002) Quantification of butyrylcholinesterase active sites in purified preparations using organophosphorus compounds. Period Biol 104(4):481–485

Kovarik Z, Radić Z, Berman HA, Simeon-Rudolf V, Reiner E, Taylor P (2004) Mutant cholinesterases possessing enhanced capacity for reactivation of their phosphonylated conjugates. Biochemistry 43:3222–3229. https://doi.org/10.1021/bi036191a

Kovarik Z, Ciban N, Radić Z, Simeon-Rudolf V, Taylor P (2006) Active site mutant acetylcholinesterase interactions with 2-PAM, HI-6, and DDVP. Biochem Biophys Res Commun 342:973–978. https://doi.org/10.1016/j.bbrc.2006.02.056

Kovarik Z, Čalić M, Šinko G, Bosak A (2007) Structure-activity approach in the reactivation of tabun-phosphorylated human acetylcholinesterase with bispyridinium para-aldoximes. Arh Hig Rada Toksikol 58:201–209. https://doi.org/10.2478/v10004-007-0013-7

Kovarik Z, Čalić M, Šinko G, Bosak A, Berend S, Lucić Vrdoljak A, Radić B (2008a) Oximes: reactivators of phosphorylated acetylcholinesterase and antidotes in therapy against tabun poisoning. Chem Biol Interact 175(1–3):173–179. https://doi.org/10.1016/j.cbi.2008.04.011

Kovarik Z, Čalić M, Bosak A, Šinko G, Jelić D (2008b) In vitro evaluation of aldoxime interactions with human acetylcholinesterase. Croat Chem Acta 81:47–57

Kovarik Z, Katalinić M, Šinko G, Binder J, Holas O, Jung Y-S, Musilova L, Jun D, Kuča K (2010a) Pseudo-catalytic scavenging: searching for a suitable reactivator of phosphorylated butyrylcholinesterase. Chem Biol Interact 187:167–217. https://doi.org/10.1016/j.cbi.2010.02.023

Kovarik Z, Katalinić M, Bosak A, Šinko G (2010b) Cholinesterase interactions with oximes. Curr Bioact Compd 6(1):9–15. https://doi.org/10.2174/157340710790711764

Kovarik Z, Maček Hrvat N, Katalinić M, Sit RK, Paradyse A, Žunec S, Musilek K, Fokin VV, Taylor P, Radić Z (2015) Catalytic soman scavenging by Y337A/F338A acetylcholinesterase mutant assisted with novel site-directed aldoximes. Chem Res Toxicol 28(5):1036–1044. https://doi.org/10.1021/acs.chemrestox.5b00060

Kovarik Z, Kalisiak J, Maček Hrvat N, Katalinić M, Zorbaz T, Žunec S, Green C, Radić Z, Fokin VV, Sharpless KB, Taylor P (2019a) Reversal of tabun toxicity enabled by a triazole-annulated oxime library—reactivators of acetylcholinesterase. Chem-Eur J 25(16):4100–4114. https://doi.org/10.1002/chem.201805051

Kovarik Z, Maček Hrvat N, Kalisiak J, Katalinić M, Sit RK, Zorbaz T, Radić Z, Fokin VV, Sharpless KB, Taylor P (2019b) Counteracting tabun inhibition by reactivation by pyridinium aldoximes that interact with active center gorge mutants of acetylcholinesterase. Toxicol Appl Pharm 372:40–46. https://doi.org/10.1016/j.taap.2019.04.007

Kovarik Z, Maček Hrvat N, Žunec S, Katalinić M (2019c) Detoxification of tabun-exposed mice by an acetylcholinesterase mutant assisted with a novel pyridinium aldoxime. Biologia Serbica 41(2):4–8. https://doi.org/10.5281/zenodo.3532038

Kryger G, Harel M, Giles K, Toker L, Velan B, Lazar A, Kronman C, Barak D, Ariel N, Shafferman A, Silman I, Sussman JL (2000) Structures of recombinant native and E202Q mutant human acetylcholinesterase complexed with the snake-venom toxin fasciculin-II. Acta Crystallogr D Biol Crystallogr 56:1385–1394. https://doi.org/10.1107/s0907444900010659

Kuhar MJ, Murrin LC (1978) Sodium-dependent, high affinity choline uptake. J Neurochem 30(1):15–21. https://doi.org/10.1111/j.1471-4159.1978.tb07029.x

Kumar A, Darreh-Shori T (2017) DMSO: a mixed-competitive inhibitor of human acetylcholinesterase. ACS Chem Neurosci 8(12):2618–2625. https://doi.org/10.1021/acschemneuro.7b00344

Lucić A, Radić B, Peraica M, Mesić M, Primožič I, Binenfeld Z (1997) Antidotal efficacy of quinuclidinium oximes against soman poisoning. Arch Toxicol 71:467–470. https://doi.org/10.1007/s002040050413

Maček Hrvat N, Zorbaz T, Šinko G, Kovarik Z (2018) The estimation of oxime efficiency is affected by the experimental design of phosphylated acetylcholinesterase reactivation. Toxicol Lett 293:222–228. https://doi.org/10.1016/j.toxlet.2017.11.022

Maraković N, Knežević A, Vinković V, Kovarik Z, Šinko G (2016) Design and synthesis of N-substituted-2-hydroxyiminoacetamides and interactions with cholinesterases. Chem Biol Interact 259(Pt B):122–132. https://doi.org/10.1016/j.cbi.2016.05.035

Masson P, Lockridge O (2010) Butyrylcholinesterase for protection from organophosphorus poisons: catalytic complexities and hysteretic behavior. Arch Biochem Biophys 494(2):107–120. https://doi.org/10.1016/j.abb.2009.12.005

Masson P, Nachon F (2017) Cholinesterase reactivators and bioscavengers for pre- and post-exposure treatments of organophosphorus poisoning. J Neurochem 142:26–40. https://doi.org/10.1111/jnc.14026

Melzer M, Heidenreich A, Dorandeu F, Gäb J, Kehe K, Thiermann H, Letzel T, Blum MM (2012) In vitro and in vivo efficacy of PEGylated diisopropyl fluorophosphatase (DFPase). Drug Test Anal 4(3–4):262–270. https://doi.org/10.1002/dta.363

Mercey G, Verdelet T, Saint-André G, Gillon E, Wagner A, Baati R, Jean L, Nachon F, Renard P-Y (2011) First efficient uncharged reactivators for the dephosphylation of poisoned human acetylcholinesterase. Chem Commun 47:5295–5297. https://doi.org/10.1039/c1cc10787a

Mosmann T (1983) Rapid colorimetric assay for cellular growth and survival: application to proliferation and cytotoxicity assays. J Immunol Methods 65:55–63. https://doi.org/10.1016/0022-1759(83)90303-4

Mukherjee S, Bapat AP, Hill MR, Sumerlin BS (2014) Oximes as reversible links in polymer chemistry: dynamic macromolecular stars. Polym Chem 5(24):6923–6931. https://doi.org/10.1039/c4py01282h

Nachon F, Brazzolotto X, Trovaslet M, Masson P (2013) Progress in the development of enzyme-based nerve agent bioscavengers. Chem Biol Interact 206(3):536–544. https://doi.org/10.1016/j.cbi.2013.06.012

Ngamelue MN, Homma K, Lockridge O, Asojoa OA (2007) Crystallization and X-ray structure of full-length recombinant human butyrylcholinesterase. Acta Crystallogr Sect F Struct Biol Cryst Commun 63:723–727. https://doi.org/10.1107/S1744309107037335

Odžak R, Primožič I, Tomić S (2007a) 3-Amidoquinuclidine derivatives: synthesis and interaction with butyrylcholinesterase. Croat Chem Acta 80:101–107. https://doi.org/10.1016/j.bioorg.2006.01.004

Odžak R, Čalić M, Hrenar T, Primožič I, Kovarik Z (2007b) Evaluation of monoquaternary pyridinium oximes potency to reactivate tabun-inhibited human acetylcholinesterase. Toxicology 233(1–3):85–96. https://doi.org/10.1016/j.tox.2006.08.003

Primožič I, Hrenar T, Tomić S (2012) Binding modes of quinuclidinium esters to butyrylcholinesterase. Croat Chem Acta 85:77–83. https://doi.org/10.5562/cca2060

Primožič I, Hrenar T, Baumann K, Krišto L, Križić I, Tomić S (2014) Mechanochemical and conformational study of *N*-heterocyclic carbonyl-oxime transformations. Croat Chem Acta 87:155–162. https://doi.org/10.5562/cca2476

Radić B, Primožič I, Mesić M, Lucić A, Binenfeld Z (1995) Quinuclidinium oximes as antidotes against soman poisoning. In: Proceedings 5th International Symposium Protection Against Chemical and Biological Warfare Agents: Suppl. 252, Stockholm, Sweden

Radić Z, Dale T, Kovarik Z, Berend S, Garcia E, Zhang L, Amitai G, Green C, Radić B, Duggan BM, Ajami D, Rebek J, Taylor P (2013a) Catalytic detoxification of nerve agent and pesticide organophosphates by butyrylcholinesterase assisted with non-pyridinium oximes. Biochem J 450(1):231–242. https://doi.org/10.1042/BJ20121612

Radić Z, Sit RK, Garcia E, Zhang L, Berend S, Kovarik Z, Amitai G, Fokin VV, Sharpless KB, Taylor P (2013b) Mechanism of interaction of novel uncharged, centrally active reactivators with OP-hAChE conjugates. Chem Biol Interact 203(1):67–71. https://doi.org/10.1016/j.cbi.2012.08.014

Radman Kastelic A, Odžak R, Pezdirc I, Sović K, Hrenar T, Čipak Gašparović A, Skočibušić M, Primožič I (2019) New and potent quinuclidine based antimicrobial agents. Molecules 24(14):2675–2692. https://doi.org/10.3390/molecules24142675

Reiner E, Škrinjarić-Špoljar M, Dunaj S, Simeon-Rudolf V, Primožič I, Tomić S (1999) 3-Hydroxyquinuclidinium derivatives: synthesis of compounds and inhibition of acetylcholinesterase. Chem Biol Interact 119–120:173–181. https://doi.org/10.1016/s0009-2797(99)00026-5

Reiner E, Bosak A, Simeon-Rudolf V (2004) Activity of cholinesterases in human whole blood measured with acetylthiocholine as substrate and ethopropazine as selective inhibitor of plasma butyrylcholinesterase. Arh Hig Rada Toksikol 55(1):1–4

Renou J, Mercey G, Verdelet T, Păunescu E, Gillon E, Arboléas M, Loiodice M, Kliachyna M, Baati R, Nachon F, Jean L, Renard P-Y (2013) Syntheses and in vitro evaluations of uncharged reactivators for human acetylcholinesterase inhibited by organophosphorus nerve agents. Chem Biol Interact 203:81–84. https://doi.org/10.1016/j.cbi.2012.09.023

Saxena A, Sun W, Luo C, Myers TM, Koplovitz I, Lenz DE, Doctor BP (2006) Bioscavenger for protection from toxicity of organophosphorus compounds. J Mol Neurosci 30:145–148. https://doi.org/10.1385/jmn:30:1:145

Saxena A, Sun W, Fedorko JM, Koplovitz I, Doctor BP (2011) Prophylaxis with human serum butyrylcholinesterase protects guinea pigs exposed to multiple lethal doses of soman or VX. Biochem Pharmacol 81(1):164–169. https://doi.org/10.1016/j.bcp.2010.09.007

Simeon-Rudolf V, Reiner E, Škrinjarić-Špoljar M, Radić B, Lucić A, Primožič I, Tomić S (1998) Quinuclidinium-imidazolium compounds: synthesis, mode of interaction with acetylcholinesterase and effect upon soman intoxicated mice. Arch Toxicol 72:289–295. https://doi.org/10.1007/s002040050504

Singh N, Karpichev Y, Gupta B, Satnami ML, Marek J, Kuca K, Ghosh KK (2013) Physicochemical properties and supernucleophilicity of oxime-functionalized surfactants: hydrolytic catalysts toward dephosphorylation of di- and triphosphate esters. J Phys Chem B 117(14):3806–3817. https://doi.org/10.1021/jp310010q

Šinko G, Katalinić M, Kovarik Z (2006) para- and ortho-pyridinium aldoximes in reaction with acetylthiocholine. FEBS Lett 580:3167–3172. https://doi.org/10.1016/j.febslet.2006.04.070

Šinko G, Brglez J, Kovarik Z (2010) Interactions of pyridinium oximes with acetylcholinesterase. Chem Biol Interact 187:172–176. https://doi.org/10.1016/j.cbi.2010.04.017

Sit RK, Fokin VV, Amitai G, Sharpless KB, Taylor P, Radić Z (2014) Imidazole aldoximes effective in assisting butyrylcholinesterase catalysis of organophosphate detoxification. J Med Chem 57(4):1378–1389. https://doi.org/10.1021/jm401650z

Sit RK, Kovarik Z, Maček Hrvat N, Žunec S, Green C, Fokin VV, Sharpless KB, Radić Z, Taylor P (2018) Pharmacology, pharmacokinetics and tissue disposition of zwitterionic hydroxyiminoacetamido alkylamines as reactivating antidotes for organophosphate exposure. J Pharmacol Exp Ther 367(2):363–372. https://doi.org/10.1124/jpet.118.249383

Skočibušić M, Odžak R, Štefanić Z, Križić I, Krišto L, Jović O, Hrenar T, Primožič I, Jurašin D (2016) Structure-property relationship of quinuclidinium surfactants—towards multifunctional biologically active molecules. Colloid Surface B 140:548–559. https://doi.org/10.1016/j.colsurfb.2015.11.023

Sterling GH, Doukas PH, Ricciardi FJ Jr, O'Neill JJ (1991) Quaternary and tertiary quinuclidine derivatives as inhibitors of choline uptake. J Pharm Sci 80:785–789. https://doi.org/10.1002/jps.2600800817

Sterling GH, Doukas PH, Jackson C, Caccese R, O'Neill JJ (1993) 3-carbamyl-*N*-allylquinuclidinium bromide. Effects on cholinergic activity and protection against soman. Biochem Pharmacol 45:465–472. https://doi.org/10.1016/0006-2952(93)90084-a

Sternbach LH, Kaiser S (1952) Antispasmodics. I. Bicyclic basic alcohols. J Am Chem Soc 74:2215–2218. https://doi.org/10.1021/ja01129a019

Timperley CM, Forman JE, Abdollahi M, Al-Amri AS, Baulig A, Benachour D, Borrett V, Cariño FA, Geist M, Gonzalez D et al (2019) Advice on assistance and protection provided by the scientific advisory board of the organisation for the prohibition of chemical weapons: part 1. On medical care and treatment of injuries from blister and nerve agents. Toxicology 415:56–69. https://doi.org/10.1515/pac-2018-0803

Vale JA, Marrs TC, Maynard RL (2018) Novichok: a murderous nerve agent attack in the UK. Clin Toxicol (Phila) 56(11):1093–1097. https://doi.org/10.1080/15563650.2018.1469759

Vučinić S, Zlatković M, Antonijević B, Ćurčić M, Bošković B (2013) Fresh frozen plasma as a successful antidotal supplement in acute organophosphate poisoning. Arh Hig Rada Toksikol 64(2):87–91. https://doi.org/10.2478/10004-1254-64-2013-2378

Wilkening S, Stahl F, Bader A (2003) Comparison of primary human hepatocytes and hepatoma cell line HepG2 with regard to their biotransformation properties. Drug Metab Dispos 31(8):1035–1042. https://doi.org/10.1124/dmd.31.8.1035

Wille T, von der Wellen J, Thiermann H, Worek F (2019) Pseudocatalytic scavenging of the nerve agent VX with human blood components and the oximes obidoxime and HI-6. Arch Toxicol 91(3):1309–1318. https://doi.org/10.1007/s00204-016-1776-x

Winter M, Wille T, Musilek K, Kuca K, Thiermann H, Worek F (2016) Investigation of the reactivation kinetics of a large series of bispyridinium oximes with organophosphate-inhibited human acetylcholinesterase. Toxicol Lett 244:136–142. https://doi.org/10.1016/j.toxlet.2015.07.007

Worek F, Widmann R, Knopff Szinicz L (1998) Reactivating potency of obidoxime, pralidoxime, HI 6 and HLö 7 in human erythrocyte acetylcholinesterase inhibited by highly toxic organophosphorus compounds. Arch Toxicol 72:237–243. https://doi.org/10.1007/s002040050495

Zorbaz T, Braïki A, Maraković N, Renou J, de la Mora E, Maček Hrvat N, Katalinić M, Silman I, Sussman JL, Mercey G, Gomez C, Mougeot R, Pérez B, Baati R, Nachon F, Weik M, Jean L, Kovarik Z, Renard PY (2018a) Potent 3-hydroxy-2-pyridine aldoxime reactivators of organophosphate-inhibited cholinesterases with predicted blood-brain barrier penetration. Chem-Eur J 24(38):9675–9691. https://doi.org/10.1002/chem.201801394

Zorbaz T, Malinak D, Maraković N, Maček Hrvat N, Zandona A, Novotny M, Skarka A, Andrys R, Benkova M, Soukup O, Katalinić M, Kuca K, Kovarik Z, Musilek K (2018b) Pyridinium oximes with ortho-positioned chlorine moiety exhibit improved physicochemical properties and efficient reactivation of human acetylcholinesterase Inhibited by several nerve agents. J Med Chem 61(23):10753–10766. https://doi.org/10.1021/acs.jmedchem.8b01398

Zorbaz T, Malinak D, Kuča K, Musilek K, Kovarik Z (2019) Butyrylcholinesterase inhibited by nerve agents is efficiently reactivated with chlorinated pyridinium oximes. Chem Biol Interact 307:16–20. https://doi.org/10.1016/j.cbi.2019.04.020